Collision free path planning of autonomous systems using novel Artificial Potential Field-based algorithm

Project-II (AE) report submitted to

Indian Institute of Technology Kharagpur

in partial fulfilment for the award of the degree of

Bachelor of Technology

in

Aerospace Engineering

by

Paridhi D Choudhary

(21AE3AI02)

Under the supervision of

Professor Manoranjan Sinha

Department of Aerospace Engineering

Indian Institute of Technology Kharagpur

Spring Semester, 2024-25

April 16, 2025

DECLARATION

I certify that

(a) The work contained in this report has been done by me under the guidance of my supervisor.

(b) The work has not been submitted to any other Institute for any degree or diploma.

(c) I have conformed to the norms and guidelines given in the Ethical Code of Conduct of the Institute.

(d) Whenever I have used materials (data, theoretical analysis, figures, and text) from other sources, I have given due credit to them by citing them in the text of the thesis and giving their details in the references. Further, I have taken permission from the copyright owners of the sources, whenever necessary.

Paridhi D Choudhary

Date: April 16, 2025 (Paridhi D Choudhary)
Place: Kharagpur (21AE3AI02)

DEPARTMENT OF AEROSPACE ENGINEERING

INDIAN INSTITUTE OF TECHNOLOGY KHARAGPUR

KHARAGPUR - 721302, INDIA

CERTIFICATE

This is to certify that the project report entitled "**Collision free path planning of autonomous systems using novel Artificial Potential Field-based algorithm**" submitted by **Paridhi D Choudhary** (Roll No. 21AE3AI02) to Indian Institute of Technology Kharagpur towards partial fulfilment of requirements for the award of degree of Bachelor of Technology in Aerospace Engineering is a record of bona fide work carried out by him under my supervision and guidance during Spring Semester, 2024-25.

Date: April 16, 2025
Place: Kharagpur

Professor Manoranjan Sinha
Department of Aerospace Engineering
Indian Institute of Technology Kharagpur
Kharagpur - 721302, India

Abstract

Name of the student: **Paridhi D Choudhary** Roll No: **21AE3AI02**
Degree for which submitted: **Bachelor of Technology**
Department: **Department of Aerospace Engineering**
Thesis title: **Collision free path planning of autonomous systems using novel Artificial Potential Field-based algorithm**
Thesis supervisor: **Professor Manoranjan Sinha**
Month and year of thesis submission: **April 16, 2025**

With the surge in space exploration missions, there is a growing accumulation of space debris orbiting the earth. This poses a growing risk of collision of the operational satellites and future space missions. To counter these risks, the development of an effective and precise guidance law for satellites is essential. Various guidance algorithms have been explored in the literature including, the Artificial Potential Field-based guidance algorithm (APF) which is widely used for real-time path adjustments to avoid the collision. However, this algorithm is prone to local minima near obstacles. To tackle with this local minima issue, many methods are available in literature, one of which has been used in this thesis (Rafal Szczepanski), modeling the spacecraft as a rigid body in Lie Space (Lee) and using Sliding Mode Controller (smc) to control the spacecraft to reach the desired goal. Furthermore, a novel Physics Informed APF (P-APF) is proposed and combined with SMC to enhance obstacle avoidance capabilities. Owing to the complex Spacecraft Dynamics, the influence of APF on spacecraft trajectory was not as profound. Consequently, the traditional APF is implemented along with a robust Model Predictive Controller for path planning and collision-avoidance of a quadrotor. Additionally, a novel Discrete APF (D-APF) is developed to address local minima issues in this setup. Simulation results validating the proposed approaches are presented.

Acknowledgements

This project owes its inception and development to the profound inspiration derived from Professor Manoranjan Sinha. His visionary insights, unwavering support, and invaluable guidance have been instrumental in shaping every facet of this endeavor. I am profoundly grateful for his mentorship, which has not only enriched the project but also significantly contributed to my personal and professional growth.

As a student studying Aerospace Engineering at the Indian Institute of Technology, Kharagpur, I extend our gratitude and appreciation towards the teaching faculty of the Aerospace Engineering Department for helping me reach where I am today and for putting up with my queries. I also appreciate our fellow batch mates for their assistance over the past few years.

To Mr. Rakesh Kumar Sahoo, who served as a mentor, I extend my deepest gratitude for his insightful suggestions and constructive feedback throughout the project, helping me and supporting me whenever I required.

To everyone involved, for all of their kind cooperation during this project, in each aspect of its work, we extend to you our thanks.

Finally, I must express my very profound gratitude to my parents for providing me with unfailing support and continuous encouragement throughout my years of study and through the process of researching and writing this thesis. This accomplishment would not have been possible without them. Thank you.

Contents

List of Figures

Chapter 1

Introduction

As spacecraft rendezvous and docking missions become increasingly complex, the need for advanced guidance laws has surged. Vital to ensuring secure rendezvous and docking of spacecraft is the task of obstacle and collision avoidance. A huge amount of additional debris is created as the cause of a major collision, thereby making collision avoidance absolutely necessary.

A lot of work has been done in the field of developing path planning algorithms with a proper balance of complexity and computational expense with robustness and performance of the solution. Analytical methods including glideslope, artificial potential function and Lyapunov functions are often used. These methods, though computationally inexpensive , don't produce optimal results, hence, the trend is to either use pure optimal methods, which though produce optimal results but are computationally expensive or to use these methods with a modification to produce relatively better results. In recent years, techniques involving use of Reinforcement Learning to tackle spacecraft rendezvous guidance challenges have been in prominent use. (rl) describes one such method. (rl) also utilises a similar approach for safe rendezvous and docking with dynamic obstacle avoidance.

Artificial Potential Field Algorithm is a popular choice among analytical path planning methods, which primarily works by assigning a repulsive potential to obstacles and an attractive potential to goal. This method is straightforward and computationally easy to implement, however, fails to give optimal results due to local minima issue. Quite a lot of variations of this algorithm have been employed to avoid local minima. (R. Szczepanski and Tarczewski) uses an an augmented reality approach, while (10) uses Reinforcement Learning to solve the same issue. Smoothness improvement was proposed in (J. Song and Su) and (Lin and Tsukada).

We have proposed a guidance algorithm to address the limitations of traditional collision avoidance techniques, particularly the local minima issues in standard APF methods.

To overcome these limitations, this thesis proposes two novel modifications to traditional APF methods. First, a Physics-Informed Artificial Potential Field (P-APF) algorithm based on the Hamiltonian principle is developed and integrated with a Sliding Mode Controller (SMC) for spacecraft modeled using Lie Group (SE(3)) dynamics. Second, a Discrete Artificial Potential Field (D-APF) approach is introduced using Delaunay Triangulation, and is implemented on a quadrotor system in conjunction with a Model Predictive Controller (MPC).

These contributions build upon the work completed in BTP-I, where the Adaptive Safe Artificial Potential Field (ASAPF) algorithm (Rafal Szczepanski) was implemented with an SMC on a spacecraft modeled as a rigid body in SE(3). Chapter 3 of this report provides a summary of the previous work, forming the foundation for the extended methods proposed and analyzed in the current phase.

Chapter 2

Literature Review

2.1 Spacecraft Modeling using Lie Algebra and Control using SMC

In the context of spacecraft control, Lie algebra is often used to analyze and control the relative movements between spacecraft in a leader-follower setup. By applying Lie algebra, one can formulate the dynamics of each spacecraft in a way that respects the geometric constraints of rotational and translational motion, which is particularly useful when dealing with coupled systems. The use of Lie algebra enables the decomposition of complex dynamics into simpler components, making it easier to design control laws that ensure stability and synchronization among spacecraft.

The paper (Lee) ,applies Lie algebra within a coupled tracking control strategy for multiple spacecraft systems. A sliding mode control (SMC) framework is employed to achieve robust tracking of a leader spacecraft by several followers, even under input saturation constraints. The control strategy is designed to ensure that the followers maintain a specified formation around the leader by using sliding mode principles to handle uncertainties and disturbances. Lie algebra in this context is instrumental in formulating the relative dynamics between the leader and followers, allowing the authors to construct a control law that respects the geometric constraints and actuator limits of each spacecraft.

The aim of this work, however, is to model the spacecraft using SE3 dynamics and to use a new approach of Artificial Potential Field Algorithm in order to ensure collision free navigation of spacecraft for rendezvous and docking purposes. Hence, only one spacecraft is modeled using this dynamics and then sliding mode controller is used to reach a desired orientation. The detailed dynamics and implementation procedure along with the simulation results are shown in Chapter 4.

Sliding Mode Controller (SMC) A sliding mode controller (SMC) is a prominent nonlinear controller that brings the state of the system from any arbitrary position to the equilibrium position. Rather than using a continuous control law, SMC traditionally uses discontinuous law for sliding around the designed sliding manifold depicted below:

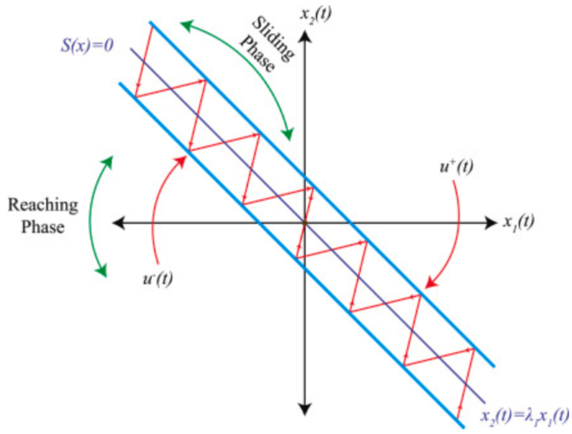

(a) (smc)

FIGURE 2.1: Sliding Mode Controller

In sliding mode control (SMC), the state-feedback control law is characterized by its switching between different continuous structures, rather than being a continuous function over time. This makes SMC a type of variable structure control. The control law is crafted to ensure that the system's trajectory continuously moves toward adjacent regions with distinct control structures, leading to a transition across multiple control structures rather than staying within a single one. Consequently, the system "slides" along the boundaries of these control regions, a behavior termed as the sliding mode. These boundaries, defining the sliding motion, are referred to as the sliding (hyper)surface. In contemporary control theory, an SMC-governed system can be viewed as a hybrid dynamical system, as it operates in a continuous state space while alternating between discrete control modes. Since it is a non linear controller, a Lyapunov stability has to be applied to keep the non linear system under control.

2.2 Quadrotor Dynamics along with Model Predictive Controller

The quadrotor is modeled using a standard 6-degree-of-freedom (6-DOF) rigid body model, incorporating both translational and rotational dynamics. The translational motion is governed by Newton's second law, while the rotational motion is captured using Euler's rotational equations. This modeling approach is widely adopted in aerial robotics literature due to its balance of fidelity and computational tractability.

2.2.1 Model Predictive Controller (MPC)

Model Predictive Control (MPC) is a control technique that computes optimal control actions by solving a constrained optimization problem at each time step. Due to its ability to handle multi-variable systems and explicitly incorporate system constraints, MPC has been extensively applied to quadrotor control for trajectory tracking and obstacle avoidance tasks. In the current work, the Artificial Potential Field (APF) algorithm is used to generate a reference trajectory that ensures obstacle avoidance. This trajectory is subsequently tracked by the quadrotor using MPC, enabling smooth and constraint-aware path following.

2.3 Artificial Potential Field Algorithm

Artificial Potential Field Algorithm has been in popular use for various path planning algorithms since past couple of years. This algorithm primarily employs an artificial potential field to regulate a robot in a certain space. It assigns an artificial potential field to every point in the world using defined potential field functions. The potential field generates attractive or repulsive forces, and the robot or the UAV is pulled towards certain points in the environment due to attractive forces or pushed away from certain points due to the repulsive forces. Obstacles produce a repulsive force while the goal produces an attractive force on the robot. Although straightforward to understand and implement, this method poses a major problem of local minima.

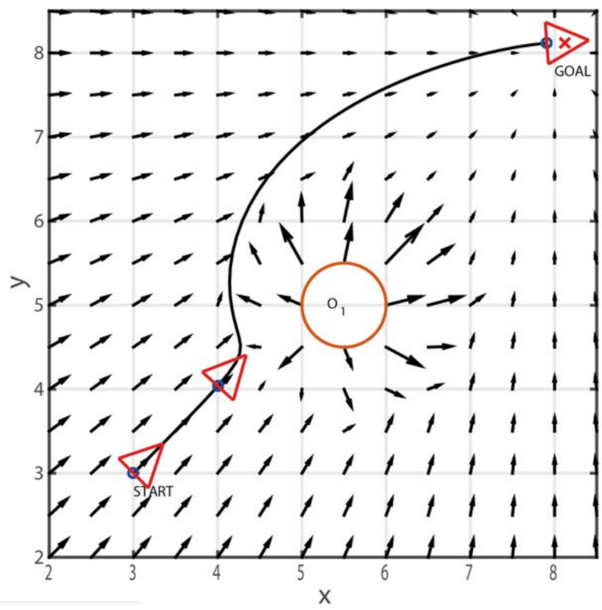

(a) (apf)

FIGURE 2.2: Artificial Potential Field Algorithm

2.3.1 Local Minima Problem

Situations in which problem of local minima is faced can majorly be categorised into three cases. First, when the robot, obstacle and goal are along the same line, obstacle being between the goal and the robot. In this case, the attractive force may be equal to the repulsive force, thereby making the total force negligible, due to which the robot might stop or hit the obstacle. Second, when the goal is in front of the robot and there are two obstacles on the left and right sides of the robot, forming a narrow passage, due to which there is a balance of net force, trapping the robot. Third, in situations when the goal is placed in between the range of obstacles, due to which the repulsive field rapidly increases, while the attractive field decreases as the robot moves towards the goal as elucidated in 2.3(a).

2.4 Delaunay Triangulation

The Artificial Potential Field (APF) is a computationally efficient collision-avoidance guidance algorithm but it is prone to local minima issue as illustrated above where attractive and repulsive force acting on the satellite balances out. To address this issue, a

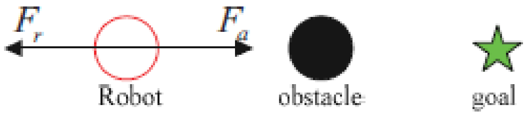

(a) (Li Zhou)

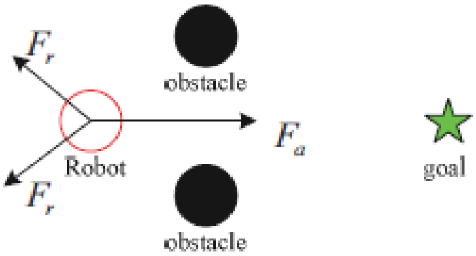

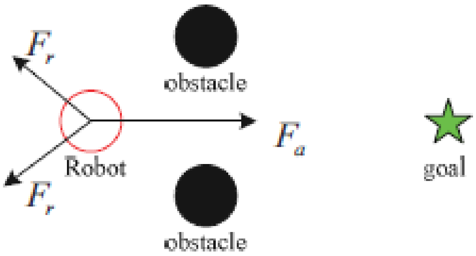

FIGURE 2.3: Artificial Potential Field Algorithm

Discrete APF (D-APF) Algorithm integrated with Delaunay Triangulation method is proposed in this paper. Delaunay triangulation is a geometric-based approach used to divide a set of points in a plane into non-overlapping triangles, ensuring no other points lie within the circumcircle of each triangle as shown in Fig. 2.4(a)

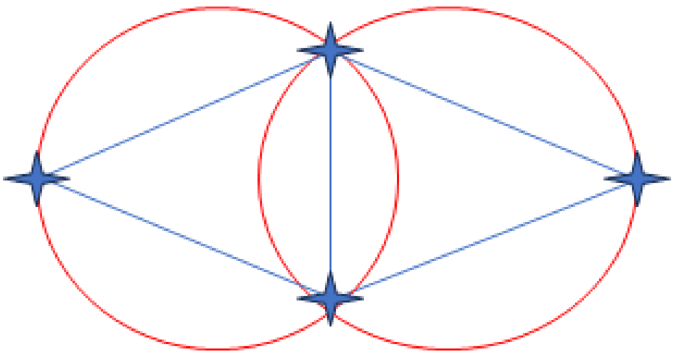

(a) (apf)

FIGURE 2.4: Delaunay Triangulation

2.5 Hamiltonian Principle (Principle of Stationary Action)

The Hamiltonian principle states that the actual path taken by a physical system between two states is the one for which the action integral is stationary or minimum. Mathematically, the action S is defined as:

$$S = \int_{t_0}^{t_f} L(q, \dot{q}, t)\, dt$$

where L is the Lagrangian of the system defined as the difference between the kinetic and potential energies, i.e.

$$L = K - U$$

where K = the kinetic energy, U = the potential energy, q = generalized coordinates, $\dot{q}$ = time derivatives of generalized coordinates. According to Hamiltonian Principle, the system follows the path which makes the variation of the action zero.

Chapter 3

Previous Work

3.1 Dynamics Modeling and Sliding Mode Controller

The spacecraft is modeled as rigid body using Lie Algebra and following a leader follower approach.

3.1.1 Leader Dynamics

The Leader spacecraft is modeled as a rigid spacecraft orbiting the Earth with its central gravity field. The configuration space of leader is SE(3). The leader attitude is represented by the rotation matrix $R^0 \in \mathrm{SO}(3)$ that transforms the leader body-fixed frame to the Earth-centered inertial (ECI) frame. The overall dynamics of the leader in compact form are given as follows:

$$I_0\dot{\xi}_0 = \mathrm{ad}^*_{\xi_0} I_0 \xi_0 + \varphi^0_g$$

Here ^{0} notation refers to the states of leader. g^0 refers to the configuration of the leader on SE(3) which is represented by the subsequent $4X4$ matrix:

$$g_0 = \begin{pmatrix} R_0 & b_0 \\ 0 & 1 \end{pmatrix}$$

while the vector of velocities of the body are:

$$\xi_0 = \begin{pmatrix} \omega^0 \\ v^0 \end{pmatrix}$$

where the leader's position is given by the inertial position vector $\mathbf{b}_0 \in \mathbb{R}^3$, representing the position from the origin of the Earth-Centered Inertial (ECI) frame to the center of mass of the leader. The translational and angular velocities of the leader are represented by the vectors $\nu_0 \in \mathbb{R}^3$ and $\mathbf{\Omega}_0 \in \mathbb{R}^3$, respectively, as observed in the leader's body-fixed frame.

Subsequently, the kinematics of the leader will be expressed as

$$\dot{g}_0 = g_0(\xi_0)^\vee$$

where

$$(\xi_0)^\vee = \begin{pmatrix} (\Omega_0)_\times & \nu_0 \\ 0 & 0 \end{pmatrix} \in \mathfrak{se}(3)$$

The mass and inertia properties of the leader, a 6×6 matrix, and the vector of gravitational forces and moments, a 6×1 vector, are expressed as

$$\phi_0^g = \begin{pmatrix} M_0^g \\ F_0^g \end{pmatrix} \in \mathbb{R}^6$$

and

$$I_0 = \begin{pmatrix} J_0 & 0 \\ 0 & m_0 I \end{pmatrix} \in \mathbb{R}^{6\times 6}$$

$$\mathrm{ad}_{\xi_0} = \begin{pmatrix} (\Omega_0)_\times & 0 \\ (\nu_0)_\times & (\Omega_0)_\times \end{pmatrix} \in \mathbb{R}^{6\times 6}$$

$$\mathrm{ad}_{\xi_0} = (\mathrm{ad}_{\xi_0})^T$$

3.1.2 Follower Dynamics

The configuration of the follower spacecraft is represented by the position vector $\mathbf{b} \in \mathbb{R}^3$ from the origin of the geocentric inertial frame to the center of mass, and the attitude by the rotation matrix $R \in \mathrm{SO}(3)$. The kinematics are given by

$$\dot{\mathbf{b}} = R\nu, \quad \dot{R} = R(\Omega)_\times$$

or equivalently,

$$\dot{g} = g(\xi)^\vee$$

where

$$(\xi)^\vee = \begin{pmatrix} (\Omega)_\times & \nu \\ 0 & 0 \end{pmatrix} \in \mathfrak{se}(3)$$

with $g \in \mathrm{SE}(3)$ representing the configuration, $\nu \in \mathbb{R}^3$ the translational velocity, and $\Omega \in \mathbb{R}^3$ the angular velocity of the follower in its body frame.

In compact form, the dynamics are:

$$I\dot{\xi} = \mathrm{ad}^*_\xi I\xi + \phi_g + \phi_c + \phi_d$$

where

$$\phi_g = \begin{pmatrix} M_g \\ F_g + mR^T a_{J2} \end{pmatrix} \in \mathbb{R}^6, \quad \phi_c = \begin{pmatrix} \tau_c \\ \phi_c \end{pmatrix} \in \mathbb{R}^6, \quad \phi_d = \begin{pmatrix} \tau_d \\ \phi_d \end{pmatrix} \in \mathbb{R}^6$$

and

$$I = \begin{pmatrix} J & 0 \\ 0 & mI \end{pmatrix} \in \mathbb{R}^{6\times 6}$$

where $\phi_g \in \mathbb{R}^6$ is the vector of gravity inputs, $\phi_c \in \mathbb{R}^6$ is the vector of control inputs, and $\phi_d \in \mathbb{R}^6$ represents external disturbances on the follower.

3.1.3 Relative Dynamics

Let the relative configuration between the leader and follower be $h \in \mathrm{SE}(3)$ and the desired relative configuration be $h_f \in \mathrm{SE}(3)$. The states of the follower spacecraft are denoted by $(g, \xi) \in \mathrm{SE}(3) \times \mathbb{R}^6$. The desired follower states are given by

$$g_d = g_0 h_f, \quad \xi_d = \mathrm{Ad}_{h_f^{-1}} \xi_0 \quad \text{for} \quad t \geq t_0$$

The configuration error is

$$h = g_0^{-1} g \quad \text{for} \quad t \geq t_0$$

The tracking error in exponential coordinates is

$$(\tilde{\eta})^{\vee} = \log_m[h_f^{-1}h] = \log_m[g_d^{-1}g]$$

where $\log_m : \mathrm{SE}(3) \to \mathfrak{se}(3)$ is the logarithm map. This leads to the relative configuration vector

$$\tilde{\eta} = \begin{pmatrix} \Theta \\ \beta \end{pmatrix} \in \mathbb{R}^6$$

where $\Theta \in \mathbb{R}^3$ and $\beta \in \mathbb{R}^3$ represent the attitude and position tracking errors, respectively.

The relative velocity of the follower with respect to the leader is

$$\tilde{\xi} = \xi - \mathrm{Ad}_{h^{-1}}\xi_0 = \xi - \mathrm{Ad}_{h_f^{-1}}\xi_d$$

where $h_f = g_d^{-1}g = \exp[(\tilde{\eta})^{\vee}]$.

The kinematics in exponential coordinates is given by

$$\dot{\tilde{\eta}} = G(\tilde{\eta})\tilde{\xi}$$

with

$$G(\tilde{\eta}) = \begin{pmatrix} A(\Theta) & 0 \\ T(\Theta, \beta) & A(\Theta) \end{pmatrix}$$

where $A(\Theta)$ and $T(\Theta, \beta)$ are specific functions defined as

$$A(\Theta) = I + \frac{1}{2}(\Theta)_{\times} + \frac{1 - \cos\theta}{\theta^2}(\Theta_{\times})^2, \quad T(\Theta, \beta) = \dots$$

The relative velocity can also be expressed as

$$\tilde{\xi} = \xi - \hat{\xi}, \quad \hat{\xi} = \mathrm{Ad}_h^{-1}\xi_0$$

and the relative acceleration is

$$\dot{\tilde{\xi}} = \dot{\xi} + \mathrm{ad}_{\xi}\,\mathrm{Ad}_h^{-1}\xi_0 - \mathrm{Ad}_h^{-1}\dot{\xi}_0$$

Substituting the dynamics equations yields

$$I\dot{\tilde{\xi}} = \mathrm{ad}_{\xi}^{*}I\xi + \phi_g + \phi_c + \phi_d + I[\mathrm{ad}_{\xi}\,\mathrm{Ad}_h^{-1}\xi_0 - \mathrm{Ad}_h^{-1}\dot{\xi}_0]$$

3.1.4 Sliding Mode Controller Formulation and overall Dynamics

To ensure relative pose tracking in spacecraft formation, a Sliding Mode Control (SMC) law was designed under the assumption of bounded disturbances. The control input for the follower spacecraft is:

$$\phi_{kc} = -\phi_k^g - \mathrm{ad}_{\xi_k}^* I_k \xi_k - I_k \left[\mathrm{ad}_{\xi_k} A_d(h_k^{-1})\xi_0 - A_d(h_k^{-1})\dot{\xi}_0\right] + CG(\eta_k)\xi_k - Ps_k - K\mathrm{sgn}(s_k)$$

Where $s_k = \eta_k + C\xi_k$ is the sliding surface, and C, P, and K are positive gain matrices. The gains are designed such that $k_i > F_i$, ensuring boundedness of the control law.

The feedback system achieves almost global asymptotic tracking of the desired trajectory (g_k, ξ_k). Stability is shown using the Lyapunov function:

$$V_k(\xi_k, h_k, \xi_0, \eta_k) = \frac{1}{2} s_k^T I_k s_k$$

whos derivative is negative semidefinite. The dynamics of the feedback system are described by:

$$\dot{\eta_k} = G(\eta_k)\xi_k$$

$$\dot{\xi_k} = -CG(\eta_k)\xi_k - I_k^{-1}[Ps_k + K\mathrm{sgn}(s_k)]$$

Once the sliding surface s_k converges to zero, both η_k and ξ_k approach zero, indicating that the relative configuration and velocities converge to the desired values. The control input is limited to prevent actuator saturation:

$$\phi_{cs} = \begin{cases} \phi_c & \text{if } \|\phi_c\| < \phi_m \\ \frac{\phi_m}{\|\phi_c\|}\phi_c & \text{if } \|\phi_c\| \geq \phi_m \end{cases}$$

Additionally, to avoid chattering, a continuous saturation function is used to replace the signum function in the control law:

$$\text{sat}(s_i, \epsilon) = \begin{cases} \frac{s_i}{\epsilon} & \text{if } |s_i| < \epsilon \\ \text{sgn}(s_i) & \text{if } |s_i| \geq \epsilon \end{cases}$$

Finally, the relative configuration and velocities are updated as:

$$h_k = h_k^f \exp(\eta_k^\vee)$$

$$g_k = g_0 h_k = g_0 h_k^f \exp(\eta_k^\vee)$$

$$\xi_k = \tilde{\xi_k} + A_d(h_k^{-1})\xi_0$$

This control scheme ensures that the spacecraft follows the desired trajectory while maintaining a relative configuration.

3.2 Artificial Potential Field Algorithm(APF)

The Artificial Potential Field (APF) algorithm is inspired by the behavior of electromagnetic particles: particles with identical potentials repel each other, while those with opposite potentials attract each other. Using this principle, a vehicle is attracted to the goal position while being repelled by obstacles. The potential function for APF is given by:

$$U(\mathbf{q}) = U_{att}(\mathbf{q}) + U_{rep}(\mathbf{q})$$

where: - $\mathbf{q}$ is the position of the vehicle, - $U_{att}(\mathbf{q})$ is the attractive potential function, - $U_{rep}(\mathbf{q})$ is the repulsive potential function.

The gradient of the total potential function is calculated to derive the force acting on the robot:

$$\nabla U(\mathbf{q}) = \nabla U_{att}(\mathbf{q}) + \nabla U_{rep}(\mathbf{q})$$

3.2.1 Attractive Potential Gradient

The gradient of the attractive potential $\nabla U_{att}(\mathbf{q})$ is defined as:

$$\nabla U_{att}(\mathbf{q}) = \begin{cases} \zeta(\mathbf{q} - \mathbf{q}^*) & \text{if } d_g \leq d_g^* \\ \frac{d_g^* \zeta(\mathbf{q}-\mathbf{q}^*)}{d_g} & \text{otherwise} \end{cases}$$

where: - $\mathbf{q}^*$ is the goal position, - $d(\mathbf{x}, \mathbf{y})$ is a function calculating the Euclidean distance between points, - ζ is the scaling factor of the attractive potential, - d_g^* is a threshold distance for selecting between a quadratic or conic potential, reducing the attractive force when the goal is far away, - $d_g = d(\mathbf{q}, \mathbf{q}^*)$ is the current distance to the goal.

3.2.2 Repulsive Potential Gradient

The gradient of the repulsive potential $\nabla U_{rep}(\mathbf{q})$ is the sum of gradients for each obstacle O_i in the environment:

$$\nabla U_{rep}(\mathbf{q}) = \sum_{i=1}^{N} \nabla U_{O_i}^{rep}(\mathbf{q})$$

where N is the number of obstacles. For an individual obstacle O_i, the repulsive gradient is defined as:

$$\nabla U_{O_i}^{rep}(\mathbf{q}) = \begin{cases} \eta \left(\frac{1}{Q^*} - \frac{1}{d_{O_i}} \right) \frac{1}{d_{O_i}^2} \nabla d_{O_i} & \text{if } d_{O_i} \leq Q^* \\ 0 & \text{otherwise} \end{cases}$$

where: - η is the scaling factor for the repulsive potential, - Q^* is the obstacle reaction margin within which repulsive forces act, - $d_{O_i} = d(\mathbf{q}, O_i)$ is the distance from the robot to obstacle O_i.

3.2.3 Adaptive Safe Artificial Potential Field Algorithm

The major difference between APF and Safe APF is that Safe APF switches between vortex potential general repulsive potential of APF in case of an obstacle, thereby, dealing with the issue of local minima. This adaptive Safe Artificial Potential Field (ASAPF) approach improves traditional APF by dynamically adjusting the repulsive potential scaling factor η to ensure safe navigation with a constant desired distance from obstacles. By applying an adaptive scaling factor, the spacecraft can effectively avoid obstacles without oscillations and maintain smooth, goal-directed motion, even in narrow corridors or environments with varying obstacle proximity.

3.2.3.1 Adaptive Scaling of Attractive Potential

The scaling factor of the attractive potential ζ is calculated using an assumed deceleration for goal-reaching movement, with the assumption that there are no obstacles close to the vehicle:

$$\zeta = \sqrt{\frac{2a_{max}d_g^*}{d_g^*}}$$

where a_{max} is the value of the assumed maximum deceleration.

3.2.3.2 Adaptive Scaling of Repulsive Potential

The adaptation of the repulsive potential scaling factor η is based on the Widrow-Hoff rule, a gradient-descent-based adaptation mechanism. This adaptation enables the spacecraft to maintain a safe distance d_{safe} from obstacles while preventing issues such as goal inaccessibility and excessive repulsive forces. The adaptive scaling factor is computed as follows:

$$\eta_{k+1} = \eta_k + \mu \cdot e_d \cdot d_{min} \cdot \nabla d$$

where: - η_k is the current repulsive scaling factor, - μ is the adaptation gain, - $e_d = d_{vort} - d_{min}$ is the distance error, where d_{vort} is the desired distance from the obstacle, and d_{min} is the minimum distance to any obstacle, - ∇d is the gradient of the distance to obstacles.

This adaptive rule continuously updates η to maintain the desired distance from obstacles. Additionally, to prevent large values that could overly influence vehicle motion, η is constrained within bounds:

$$\eta_{\min} \leq \eta \leq \eta_{\max}$$

where: - $\eta_{\min} = f_\eta(d_{safe}, -v_{max})$ ensures that the robot moves away with maximum velocity when at d_{safe}, - $\eta_{\max} = f_\eta(Q^* - d_{safe}, v_{max})$, ensuring the robot reaches the goal efficiently when far from obstacles.

Control Signal Computation

The ASAPF algorithm utilizes the gradient of the potential function as a velocity signal. Linear velocity v^* and orientation θ^* are adjusted using adaptive scaling for collision-free navigation:

$$v^* = \begin{cases} \min(\alpha \cdot \|\nabla U(\mathbf{q})\|, v_{max}), & \text{if } |\theta_{error}| \leq \theta_{max}^{error} \\ 0, & \text{otherwise} \end{cases}$$

$$\theta^* = \text{atan2}(-\nabla U_y(\mathbf{q}), -\nabla U_x(\mathbf{q}))$$

where: - $\alpha = \frac{\theta_{max}^{error} - |\theta_{error}|}{\theta_{max}^{error}}$ scales the velocity based on the robot's orientation error θ_{error}, - v_{max} is the maximum allowable linear velocity.

3.3 Combining Guidance Law with Dynamics

In order to utilize the ASAPF guidance law with the SE(3) Dynamics of the spacecraft along with the Sliding Mode Controller as discussed above, the total Force was taken from ASAPF and it was added in the control input of sliding mode controller ϕ_{kc}.

$$\boldsymbol{\phi}_r = \begin{bmatrix} 0 \\ 0 \\ 0 \\ \nabla U \end{bmatrix}$$

where ∇U represents the total force derived from ASAPF. The control input thus becomes:

$$\phi_{kc} = -\phi_k^g - \mathrm{ad}^*_{\xi_k} I_k \xi_k - I_k \left[\mathrm{ad}_{\xi_k} A_d(h_k^{-1})\xi_0 - A_d(h_k^{-1})\dot{\xi}_0\right] + CG(\eta_k)\xi_k - Ps_k - K\mathrm{sgn}(s_k) + \phi_r$$

The dynamics is thus changed accordingly.

3.4 Simulation Results

3.4.1 Dynamics and Sliding Mode Controller

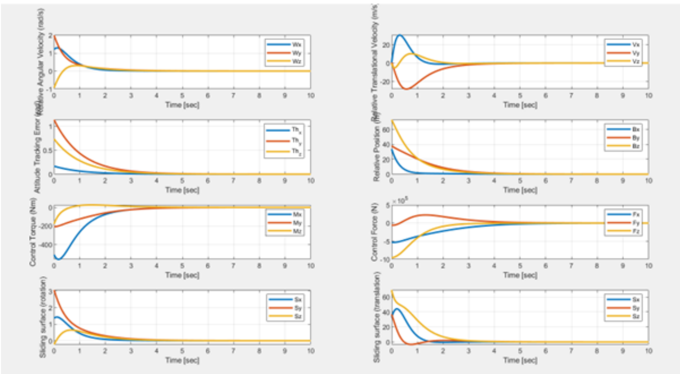

FIGURE 3.1: Dynamics and SMC simulation (Matlab)

3.4.2 Obstacle avoidance using ASAPF in 3d including Dynamics and SMC

Combining the dynamics and SMC along with ASAPF guidance law gave following results in simulation:

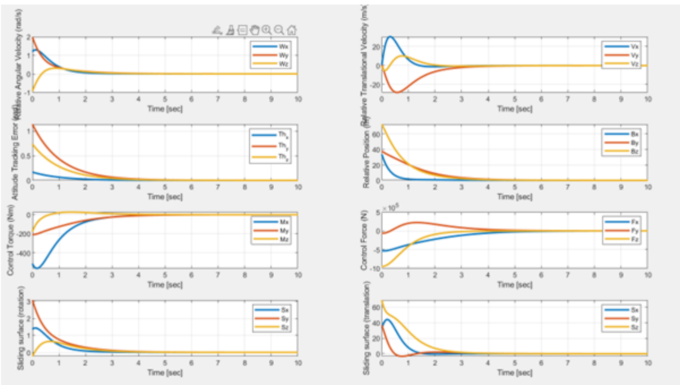

FIGURE 3.2: SMC with dynamics and Guidance Law

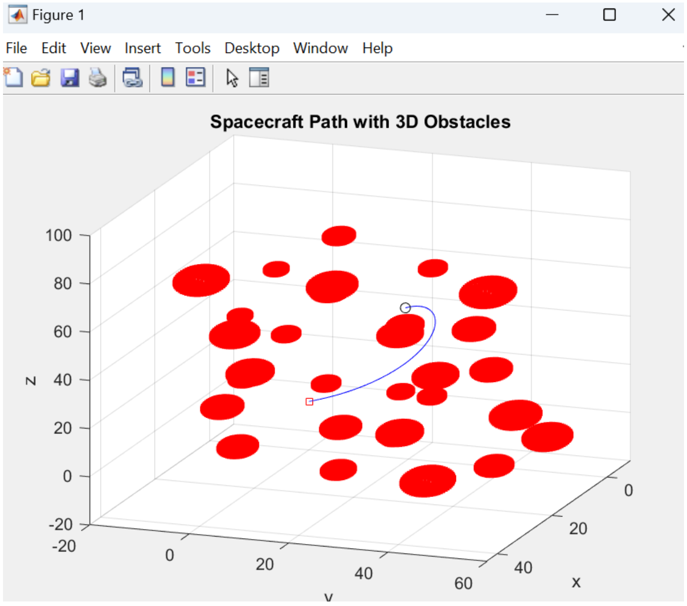

FIGURE 3.3: SMC with dynamics and Guidance Law

Chapter 4

Proposed Methodology and Implementation

This chapter outlines the proposed methodologies designed to enhance autonomous guidance and collision avoidance for two distinct platforms: spacecraft and quadrotors. Building on the foundational work established in BTP-I, the current work extends the Artificial Potential Field (APF) approach to address key limitations such as local minima and lack of physical interpretability.

Two modified APF-based strategies are developed:

- Physics-Informed APF (P-APF) for spacecraft formation control, leveraging the Hamiltonian framework and integrated with a Sliding Mode Controller (SMC) for systems evolving on SE(3).

- Discrete APF (D-APF) using Delaunay Triangulation for real-time path planning in cluttered environments, applied to quadrotor navigation alongside Model Predictive Control (MPC).

The chapter first describes the formulation of the P-APF with SMC. It then introduces the quadrotor system model, followed by a description of the MPC framework used for trajectory generation. Finally, the D-APF strategy is presented as a grid-based navigation method to overcome traditional APF challenges in dynamic obstacle settings.

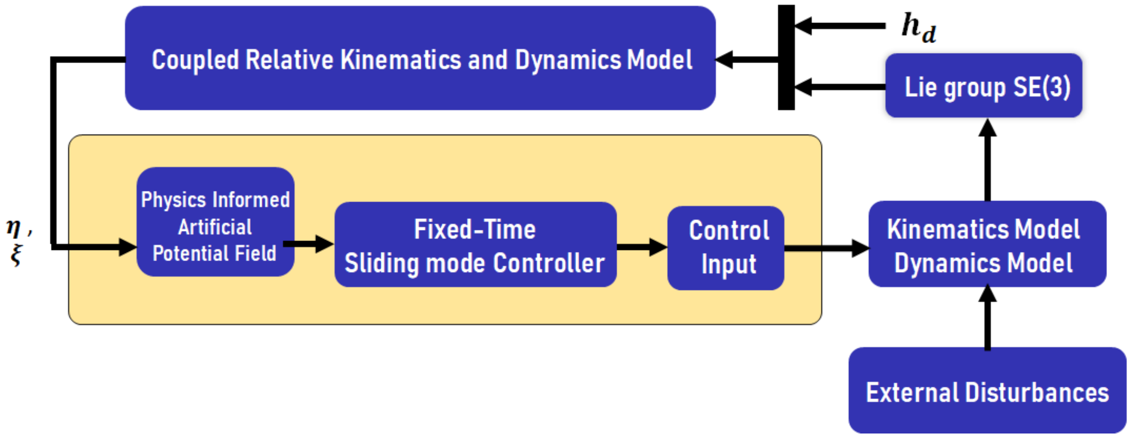

FIGURE 4.1: Proposed Control Architecture for P-APF

4.1 Spacecraft Navigation and Control using P-APF

4.1.1 Spacecraft Dynamics

The spacecraft is modeled as a rigid body using Lie Algebra, following a Leader Chaser approach, as discussed in Previous Work. The dynamics of the spacecraft remains the same as the Coupled Relative Kinematics and Dynamics Model as elucidated in Previous Work.

4.1.2 Proposed Control Architecture

Fig. 4.1 elucidates the proposed control architecture schematically. The current relative configuration and velocity errors are processed by the P-APF algorithm to generate an artificial potential-based force. This force is combined with the control input from SMC and applied to the spacecraft's kinematics and dynamics model, along with external disturbances, to yield the updated configuration and velocity states.

4.1.3 Physics- Informed Artificial Potential Field Algorithm (P-APF)

Physics - Informed Artificial Potential Field (P-APF) Algorithm derives its fundamental idea from Hamiltonian Principle as described in 2., which can be derived from traditional APF in the following way:

4.1.3.1 Traditional APF Formulation

As discussed before, APF consists of a potential function comprising of attractive potentials (for goal) and repulsive potentials (for obstacles). The expression of attractive potential is a quadratic function of relative position of chaser spacecraft w.r.t. target spacecraft (since goal is modelled as target spacecraft); i.e,

$$\tilde{U}_a = \frac{1}{2}k_a\tilde{\beta}^2$$

The expression of repulsive potential of obstacle is a function of relative position of chaser spacecraft w.r.t obstacle; i.e,

$$\tilde{U}_r = \frac{1}{2}k_r\frac{1}{d_{O_i}^2}$$

where, $\tilde{\beta}$ is relative position of chaser spacecraft w.r.t. target and d_{O_i} is the relative position of chaser spacecraft with i^{th} obstacle. The resultant APF Force is derived from the gradient of respective potential functions; i.e,

$$F_{apf} = \nabla\tilde{U}_a + \nabla\tilde{U}_b$$

$$F_{apf} = k_a\tilde{\beta} - \frac{k_r}{d_{O_i}^3}$$

Local Minima occurs when $F_{apf} = 0$.

4.1.3.2 P-APF Formulation

As seen from above, Traditional APF is a 3-DOF based Path Planning Algorithm; i.e, it gives the necessary force but not the moments, and hence, often leads to the problem of local minima. However, what is being proposed here is a 6-DOF based Path planning algorithm, based on Hamiltonian Mechanics, which provides both the necessary force and moments.

- **Attractive Artificial Potential Field for Translational Motion:** The expression of attractive static potential is a quadratic function of relative position of chaser spacecraft w.r.t target spacecraft; i.e,

$$\tilde{U}_a = \frac{1}{2}k_a\tilde{\beta}^2$$

The expression of attractive kinetic potential is a quadratic function of relative velocity of chaser spacecraft w.r.t target spacecraft; i.e,

$$\tilde{K}_a = \frac{1}{2}k_a\tilde{v}_r^2$$

Attractive Hamiltonian operator for translational motion is defined as the sum of kinetic and static potential,

$$\tilde{H}_a = \tilde{K}_a + \tilde{U}_a = \frac{1}{2k_a}\tilde{p}_a^2 + \frac{1}{2}k_a\tilde{\beta}^2$$

where $\tilde{p}_a = k_a\tilde{v}_r$ is the attractive linear momentum factor. Attractive force acting on the chaser spacecraft can be computed by solving Hamiltonian equation,

$$\dot{\tilde{p}}_a + \frac{\partial \tilde{H}_a}{\partial \tilde{\beta}} = \tilde{F}_a \Rightarrow k_a\dot{\tilde{v}}_r + k_a\tilde{\beta} = \tilde{F}_a$$

- **Repulsive Artificial Potential Field for Translational Motion:** The expression of repulsive static potential is a quadratic function of relative position of chaser satellite w.r.t obstacle,

  $$\tilde{U}_r = \frac{1}{2}k_r(\frac{1}{d_{O_i}})^2$$

  The expression of repulsive kinetic potential is a quadratic function of relative velocity of chaser spacecraft w.r.t obstacle,

  $$\tilde{K}_r = \frac{1}{2}k_r(\frac{1}{v_{O_i}})^2$$

  Repulsive Hamiltonian operator for translational motion is defined as the sum of kinetic and static potential,

  $$\tilde{H}_r = \tilde{K}_r + \tilde{U}_r = \frac{1}{2k_r}\tilde{p}_r^2 + \frac{1}{2}k_r(\frac{1}{d_{O_i}})^2$$

  where $\tilde{p}_r = \frac{k_r}{v_{O_i}}$ is the repulsive linear momentum factor. Repulsive Force acting on the chaser spacecraft can be computed by solving the Hamiltonian equation,

  $$\dot{\tilde{p}}_r + \frac{\partial \tilde{H}_r}{\partial d_{O_i}} = \tilde{F}_r \Rightarrow -\frac{k_r\dot{v}_{O_i}}{v_{O_i}^2} - \frac{k_r}{d_{O_i}^3} = \tilde{F}_r$$

- **Attractive Artificial Potential Field for Rotational Motion:** The expression of attractive static potential is a quadratic function of relative orientation of chaser spacecraft body fixed frame w.r.t target spacecraft,

$$\tilde{U}_{\theta a} = \frac{1}{2} k_a \Theta^2$$

The expression of attractive kinetic potential is a quadratic function of relative angular velocity of chaser spacecraft w.r.t target spacecraft,

$$\tilde{K}_{\theta a} = \frac{1}{2} k_a \tilde{\Omega}_r^2$$

Attractive Hamiltonian operator for translational motion is defined as the sum of kinetic and static potential,

$$\tilde{H}_{\theta a} = \tilde{K}_{\theta a} + \tilde{U}_{\theta a} = \frac{1}{2k_a} \tilde{\prod}_a^2 + \frac{1}{2} k_a \Theta^2$$

where $\tilde{\prod}_a = k_a \tilde{\Omega}_r$ is the attractive angular momentum factor. Attractive torque acting on the chaser spacecraft can be computed by solving Hamiltonian equation,

$$\dot{\tilde{\prod_a}} + \frac{\partial \tilde{H}_{\theta a}}{\partial \Theta} = \tilde{M}_a \Rightarrow k_a \dot{\tilde{\Omega}}_r + k_a \tilde{\Theta} = \tilde{M}_a$$

- **Repulsive Artificial Potential Field for Rotational Motion:** The expression of repulsive static potential is a quadratic function of relative position of chaser spacecraft w.r.t obstacle,

  $$\tilde{U}_{\theta r} = \frac{1}{2} k_r \left(\frac{1}{\Theta_{O_i}}\right)^2$$

  The expression of repulsive kinetic potential is a quadratic function of relative velocity of chaser spacecraft w.r.t obstacle,

  $$\tilde{K}_{\theta r} = \frac{1}{2} k_r \left(\frac{1}{\tilde{\Omega}_{O_i}}\right)^2$$

  Repulsive Hamiltonian operator for translational motion is defined as the sum of kinetic and static potential,

  $$\tilde{H}_{\theta r} = \tilde{K}_{\theta r} + \tilde{U}_{\theta r} = \frac{1}{2k_r} \tilde{\prod}_r^2 + \frac{1}{2} k_r \left(\frac{1}{\Theta_{O_i}}\right)^2$$

where $\tilde{\prod}_r = \frac{k_r}{\tilde{\Omega}_{O_i}}$ is the repulsive angular momentum factor. Repulsive Torque acting on the chaser spacecraft can be computed by solving the Hamiltonian equation,

$$\dot{\tilde{\prod_r}} + \frac{\partial \tilde{H}_r}{\partial \Theta_{O_i}} = \tilde{M}_r \Rightarrow -\frac{k_r \dot{\tilde{\Omega}}_{O_i}}{\tilde{\Omega}^2_{O_i}} - \frac{k_r}{\Theta^3_{O_i}} = \tilde{M}_r$$

- **Total APF Force and Moment:** Resultant force acting on chaser spacecraft to plan a collision-free path is given by, $\tilde{F}_{APF} = \tilde{F}_a + \tilde{F}_r$ Resultant moment acting on the chaser spacecraft is given by, $\tilde{M}_{APF} = \tilde{M}_a + \tilde{M}_r$

The resultant collision avoidance input vector based on P-APF is given by,

$$\tilde{\phi}_{APF} = \begin{bmatrix} \tilde{M}_{APF} \\ \tilde{F}_{APF} \end{bmatrix}$$

This is added to the control input given by SMC.

4.2 Quadrotor Control and Planning Using D-APF

4.2.1 Quadrotor Dynamics

To illustrate the 6DOF motion of the quadrotor, two frames are defined, the earth inertial frame and the body-fixed frame. The state vector can be represented as:

$$x = \begin{bmatrix} \phi & \theta & \psi & p & q & r & u & v & w & x \\ y & z \end{bmatrix}^T \in \mathbb{R}^{12}$$

The dynamic model of the quadrotor in the inertial frame is:

$$\ddot{x} = -\frac{f_t}{m}\left[\sin(\phi)\sin(\psi) + \cos(\phi)\cos(\psi)\sin(\theta)\right]$$

$$\ddot{y} = -\frac{f_t}{m}\left[\cos(\phi)\sin(\psi)\sin(\theta) - \cos(\psi)\sin(\phi)\right]$$

$$\ddot{z} = g - \frac{f_t}{m}\left[\cos(\phi)\cos(\theta)\right]$$

$$\ddot{\phi} = \frac{I_y - I_z}{I_x}\dot{\theta}\dot{\psi} + \frac{\tau_x}{I_x}$$

$$\ddot{\theta} = \frac{I_z - I_x}{I_y}\dot{\phi}\dot{\psi} + \frac{\tau_y}{I_y}$$

$$\ddot{\psi} = \frac{I_x - I_y}{I_z}\dot{\phi}\dot{\theta} + \frac{\tau_z}{I_z}$$

where f_t is the thrust, τ_x, τ_y, τ_z are the torques acting in x, y and z directions, I_x, I_y, I_z and m are the inertia and mass properties of the quadrotor.

4.2.2 Model Predictive Controller

A model predictive controller as described in (Abdellatif and El-Badawy) is designed. The MPC controller solves an optimization problem through time interval $[k, k+N]$ to predict the sequence of control inputs needed to be applied over the prediction horizon N so that the system is actuated in optimized path. Only the first control action step is applied and the rest of the steps are discarded. An optimal control problem is solved as given by:

$$\begin{aligned}
\min_{\mathbf{u},\mathbf{x}} \quad & J_N(\mathbf{x}_0, \mathbf{u}) = \sum_{k=0}^{N-1} \ell(\mathbf{x}_u(k), \mathbf{u}(k)) \\
\text{subject to} \quad & \mathbf{x}_u(k+1) = \mathbf{f}(\mathbf{x}_u(k), \mathbf{u}(k)) \\
& \mathbf{x}_u(0) = \mathbf{x}_0 \\
& \mathbf{u}(k) \in U, \quad \forall k \in [0, N-1] \\
& \mathbf{x}_u(k) \in X, \quad \forall k \in [0, N]
\end{aligned}$$

where $l(x, u)$ is the running cost function, penalizing the difference between predicted states and the reference trajectory as given by D-APF, and the difference between predicted control inputs and reference control inputs,

$$\ell(\mathbf{x}, \mathbf{u}) = \|\mathbf{x}_u - \mathbf{x}^r\|^2_{\mathbf{Q}} + \|\mathbf{u} - \mathbf{u}^r\|^2_{\mathbf{R}}$$

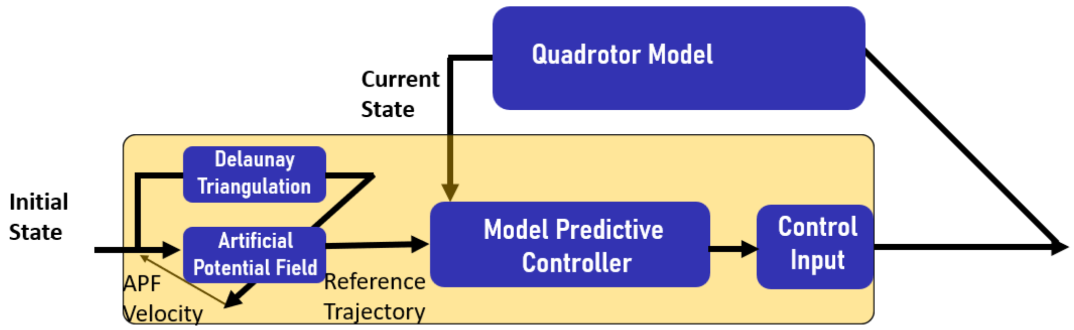

FIGURE 4.2: Proposed Control Architecture for D-APF

4.2.3 Proposed Control Architecture

Fig. 4.2 illustrates the proposed control architecture. The initial state is fed into the D-APF path planning module, which utilizes Delaunay Triangulation and Artificial Potential Fields to compute a velocity vector that ensures obstacle avoidance. This velocity is used to generate a reference trajectory. The reference trajectory is then provided to the Model Predictive Controller (MPC), which continuously minimizes the deviation between the current state and the reference trajectory. Based on this, the MPC generates appropriate control inputs that are applied to the quadrotor model. This closed-loop architecture ensures smooth and dynamically feasible trajectory generation while incorporating obstacle avoidance through discrete spatial awareness.

4.2.4 Discrete Artificial Potential Field Algorithm (D-APF)

In the proposed Discrete Artificial Potential Field (D-APF) approach, the Delaunay Triangulation method is integrated to ensure safe navigation through obstacles. Obstacles are modeled as vertices of Delaunay triangles, forming a network of interconnected triangles that define the navigable space as shown in Fig. 4.3. Instead of considering the cumulative repulsive force from all obstacles, the algorithm focuses only on the two nearest obstacles at any instant determined using delaunay triangulation based geometric method. This localized approach enhances adaptability, enabling the spacecraft to navigate narrow passages and avoid local minima more effectively.

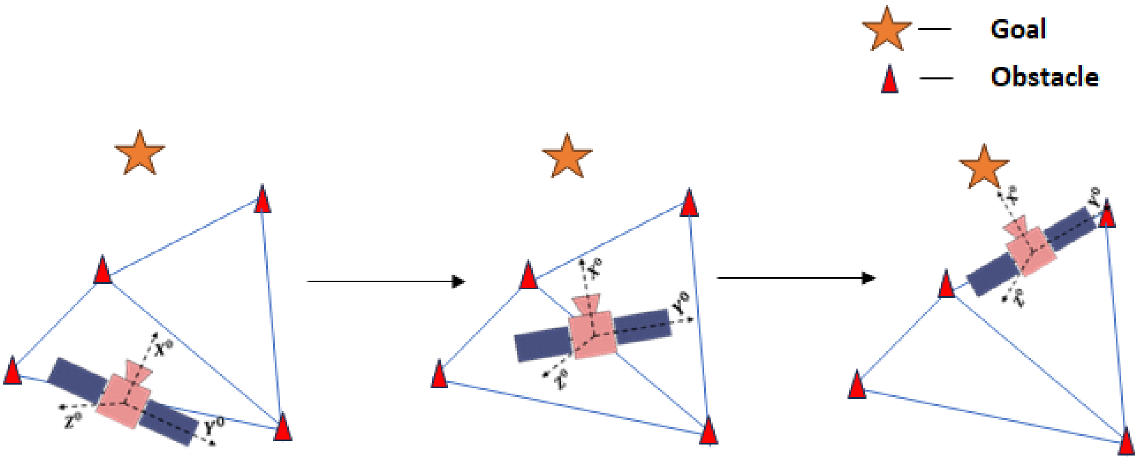

FIGURE 4.3: Illustration of spacecraft motion through Proposed D-APF

Chapter 5

Simulation Results

5.1 Obstacle avoidance of spacecraft using P-APF and SMC

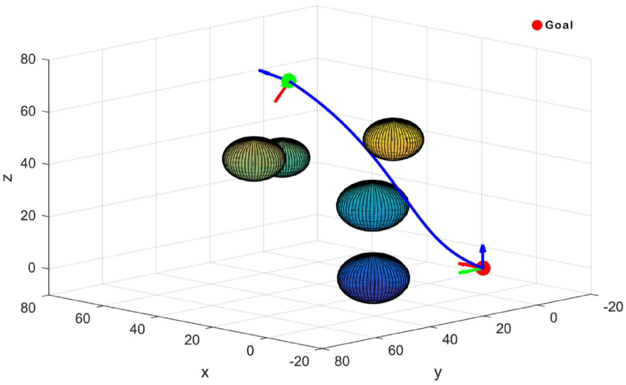

FIGURE 5.1: Illustration of collision free trajectory of spaceraft using P-APF and SMC

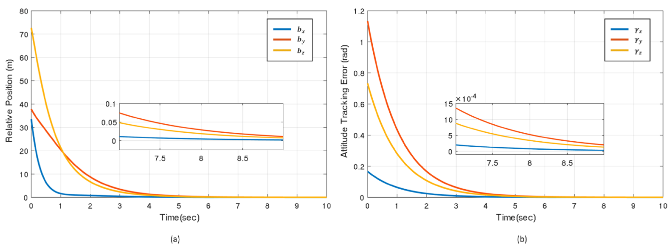

FIGURE 5.2: Plot of configuration tracking error: (a)Relative Position (b)Attitude Tracking Error

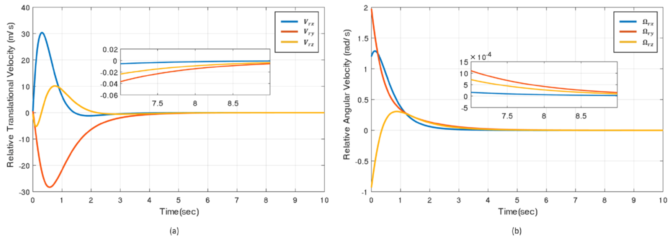

FIGURE 5.3: Plot of relative velocity: (a)Translational Velocity error (b)Angular Velocity error

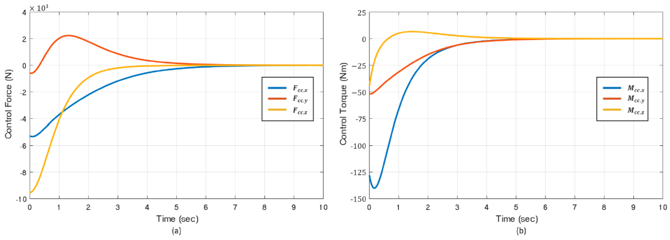

FIGURE 5.4: Plot of Control Input acting on chaser spacecraft: (a)Control Force (b)Control Torque

5.2 Obstacle avoidance on Quadrotor using D-APF and MPC

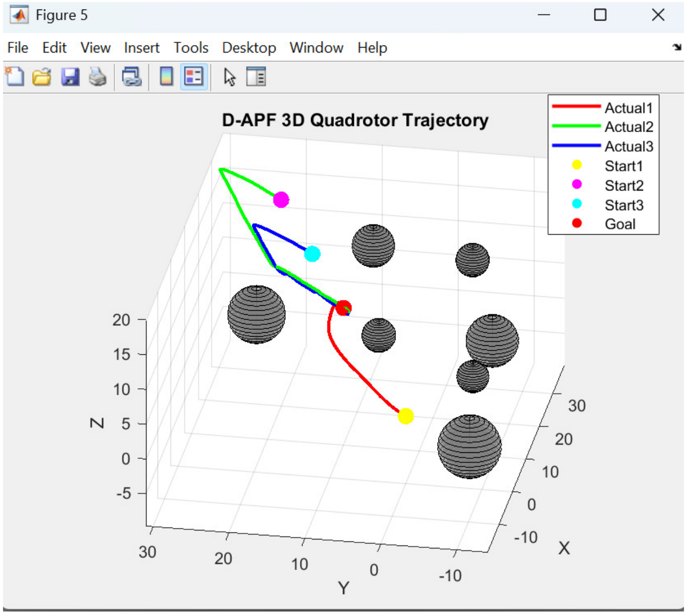

FIGURE 5.5: Illustration of collision free trajectory of quadrotor from different initial points using D-APF and MPC

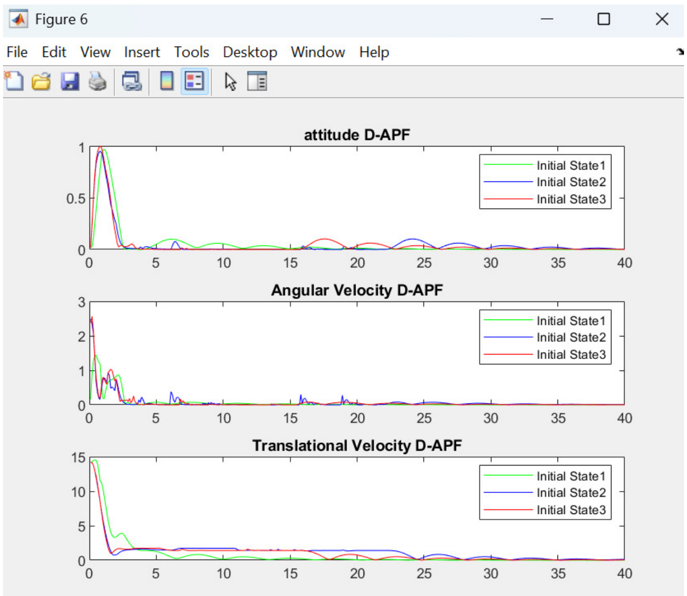

FIGURE 5.6: Plot of attitude error, angular velocity and translational velocity of quadrotor starting from different initial positions

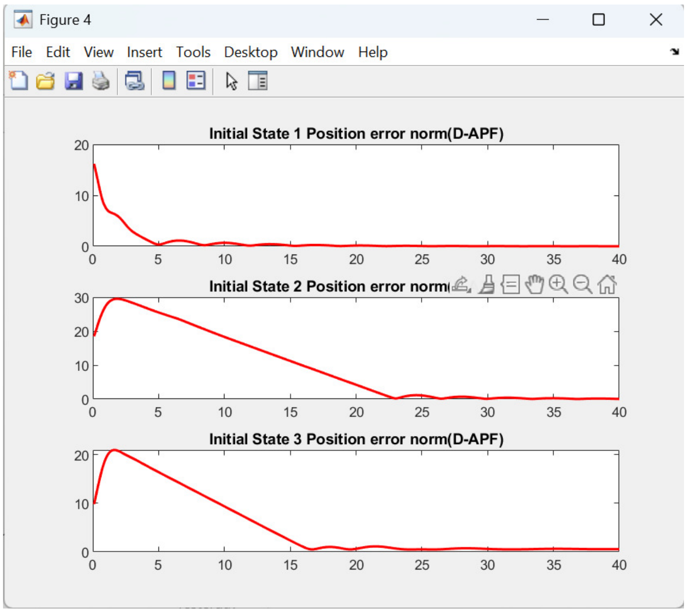

FIGURE 5.7: Plot of position error of quadrotor starting from different initial positions

Bibliography

[rl] Advancing spacecraft rendezvous and docking through safety reinforcement learning and ubiquitous learning principles author links open overlay panel. https://www.sciencedirect.com/science/article/pii/S0747563223004612?via%3Dihub.

[apf] Obstacles avoidance based on switching potential functions. https://www.researchgate.net/publication/320174864_Obstacles_Avoidance_Based_on_Switching_Potential_Functions/figures?lo=1.

[rl] Run-time assured reinforcement learning for safe spacecraft rendezvous with obstacle avoidance. https://doi.org/10.1007/978-981-99-8664-4_17.

[smc] Sliding mode controller. https://www.sciencedirect.com/topics/engineering/sliding-mode-controller.

[Abdellatif and El-Badawy] Abdellatif, R. A. and El-Badawy, A. A. Artificial potential field for dynamic obstacle avoidance with mpc-based trajectory tracking for multiple quadrotors.

[J. Song and Su] J. Song, C. H. and Su, J. Path planning for unmanned surface vehicle based on predictive artificial potential field.

[Lee] Lee, D. Spacecraft coupled tracking maneuver using sliding mode control with input saturation.

[Li Zhou] Li Zhou, W. L. Adaptive artificial potential field approach for obstacle avoidance path planning.

[Lin and Tsukada] Lin, P. and Tsukada, M. Model predictive path-planning controller with potential function for emergency collision avoidance on highway driving,.

[10] Q. Yao, Z. Zheng, L. Q. H. Y. X. G. M. Z. Z. L. and Yang, T. (2020). Path planning method with improved artificial potential field—a reinforcement learning perspective.

[R. Szczepanski and Tarczewski] R. Szczepanski, A. B. and Tarczewski, T. Efficient local path planning algorithm using artificial potential field supported by augmented reality.

[Rafal Szczepanski] Rafal Szczepanski, F. G. Local path planning algorithm based on artificial potential field with adaptive scaling factor.